

Modelling CO₂ - water mixture thermodynamics using various equations of state (EoSs) with emphasis on the potential of the SPUNG EoS

Mohamed Ibrahim^{a,*}, Geir Skaugen^b, Ivar S. Ertesvåg^a, Tore Haug-Warberg^c

^a*Department of Energy and Process Engineering, Norwegian University of Science and Technology, Kolbjørn Hejes veg 1B, NO-7491 Trondheim, Norway.*

^b*SINTEF Energy Research, Trondheim, Norway*

^c*Department of Chemical Engineering, Norwegian University of Science and Technology, Trondheim, Norway*

Abstract

CO₂-water is a very important mixture in the Carbon Capture and Storage (CCS) industry. The mixture can have a broad range of concentrations, from water as an impurity in CO₂ transport to high water concentrations in sequestration processes. CO₂-mixture is challenging due to the polar nature that induces difficulties describing the interaction between CO₂ and water when modelling the behavior. The work focus on the evaluation of the predictability of the extended corresponding state equation SPUNG in dealing with CO₂-water thermodynamics. The evaluation is done by comparing the behavior of SPUNG equation of state (EoS) to experimental data, and two other EoSs of a different class. The two other EoSs are the cubic equation Soave-Redlich-Kwong (SRK) with van der Waals mixing rules, and SRK with

*Corresponding author. Phone: +47 735 93841

Email addresses: mohamed.ibrahim@ntnu.no (Mohamed Ibrahim), Geir.Skaugen@sintef.no (Geir Skaugen), ivar.s.ertesvag@ntnu.no (Ivar S. Ertesvåg), tore.haug-warberg@ntnu.no (Tore Haug-Warberg)

Huron–Vidal mixing rules.

The predictability of the single and liquid rich phases densities, two-phase solubilities and dew line are investigated over a wide range of pressures, temperatures and mixture compositions. The results show better density prediction using SPUNG EoS over all the evaluated conditions compared to SRKs with a potential of improvements by changing the reference fluid. However, the CO₂ solubility prediction using SPUNG requires the use of other mixing rules that can account for the polar nature of the system.

Keywords: Cubic EoS, Extended Corresponding States, MBWR EoS, CCS, Reference fluid, VLE.

1. Introduction

Through the various CCS processes, CO₂ exists in mixtures with various impurities like CH₄, CO, H₂O, H₂S, N₂, NO₂ and O₂. Therefore, the knowledge of the thermophysical properties of those mixtures is a key challenge for accurate design of efficient and secure processes. Hendriks et al. (2010) pointed out the need for accurate thermophysical properties.

Even in the cases where experimental data exist for a mixture, they are discrete and local in nature, and more continuous and generic solutions are rather practical. Consequently, the modelling of the thermodynamic properties for pure CO₂ and CO₂ mixtures is a very important aspect for the analysis and detailed simulation of CCS processes. Indeed, the choice of models may have a great impact on the decisions about process design, energy efficiency, economy and safety.

A computationally cheap modelling strategy is to empirically fit experi-

mental data. This solution has a poor generality to different mixtures and for different phases and intervals outside the fitted range. A more physically profound and rather general and continuous approach is the use of Equations of State (EoSs), which will be discussed more in detail in the following section. There is a large variety of EoSs at various levels of sophistication. Cubic EoSs like Soave-Redlich-Kwong (SRK) (Soave, 1972), SRK with Huron Vidal mixing rules (SRK-HV) (Huron and Vidal, 1979) and Peng–Robinson (PR) (Peng and Robinson, 1976) are among the simplest. Multi-parameter approaches like GERG (Groupe Européen de Recherches Gazières) (Kunz et al., 2007) and Span–Wagner (Span and Wagner, 1996) are at least one order of magnitude higher in computational time. The full methods of extended corresponding states like those implemented in the REFPROP library of the National Institute of Standards and Technology (NIST) (Lemmon et al., 2010) are even more expensive than multi-parameter approaches. Among the State-of-the-art approaches are the Cubic-Plus-Association (CPA) (Kontogeorgis et al., 1996) and Statistical Associating Fluid Theory (SAFT) (Chapman et al., 1990) EoS. Tzivintzelis et al. (2011), Diamantonis and Economidis (2012) show the high success of the CPA, and Perturbed Chain SAFT (PC-SAFT) approaches in modelling polar mixtures including *COO* -Water. The two articles include a review of the development and the enormous literature on CPA, SAFT, and their different modifications and combinations, respectively.

The level of sophistication and generality usually has a direct relation to accuracy and computational complexity and, consequently, a trade-off arises. While the accuracy of a model is of higher importance than the computa-

tional efficiency for the process analysis, the computational complexity has a significant effect on the cost and feasibility of a CFD simulation. Three other dimensions of the challenge of developing or selecting a model are the generality with respect to different fluids and mixtures, consistency, and numerical stability when using it in conjunction with CFD simulations.

A consistent approach that is not well known but has shown a very good compromise in accuracy and computation time for hydrocarbons is the SPUNG EoS (Jørstad, 1993). The SPUNG EoS was not published outside Jørstad thesis before the work of (Wilhelmsen et al., 2012). The latter shows that SPUNG is a very good compromise for CO₂ with some non-polar binary and ternary impurities. Wilhelmsen et al. (2012) show that for calculations of density, enthalpy and entropy over a 10 000 random conditions in different phase regions, and for three component CO₂ mixtures, SPUNG run time was 4 times and GERG was 40 times of that of SRK. This shows the great reduction in computation time while the work shows that SPUNG accuracy is generally high compared to GERG and Span-wagner. This results was only for single phase including critical and near critical conditions, since flash results would strongly depend on algorithmic and implementation. since Since generality is an important aspect when selecting a model to be used for CFD, this work aims to study the behavior of the SPUNG EoS for the polar mixture of CO₂ and water. The study of the SPUNG EoS generality with respect to CO₂-water mixtures is of particular importance because these mixtures exists commonly in the range of processes in CCS industry. Moreover, they are very challenging mixtures due to the polar nature. A preliminary study was conducted by Ibrahim et al. (2012) that covered a few conditions that

exist in CCS. The study presented here is to extend the evaluation over a wide range of conditions, compositions, temperatures, pressures that might occur in various CCS processes. Consequently, this study can be used as a comprehensive visualized analysis of the behavior and the errors of each EoS at this wide range of conditions.

Here, an evaluation is done by comparing the behavior of SPUNG to two other EoSs and with experimental data. The two EoSs are the cubic equation SRK with the van der Waals mixing rule (Soave, 1972) and SRK-HV (Huron and Vidal, 1979).

The SRK-HV was used because it showed very good results for the solubility prediction for the investigated mixtures as reported by Austegard et al. (2006). Furthermore, The classical SRK was chosen because SPUNG use it for computing the shape factors and because it is a simple model and is commonly used in industry.

In this work, the predictability of single phase densities, dew lines, mixture solubilities in two-phase, and rich densities will be evaluated.

2. Theory

2.1. Equations of state

An EoS is a model that calculates for both the liquid and gas phase using the same expression. This enhances the continuity near the critical point. An EoS for an N_c component mixture can be regarded as an expression for pressure P as a function of the mole fractions x_i , the temperature T and the volume V . Given this expression, it can be manipulated to calculate the fugacity of each component. In the following subsections, a brief description of

the equations of state used in the work will be given together with references for further discussions.

2.2. The standard SRK

The classical SRK model (Soave, 1972) is a cubic EoS that uses van der Waals mixing rules.

2.3. The SRK Model with Huron–Vidal mixing rules

This model, proposed by Huron and Vidal (1979), is an improvement from the classical SRK, as it derives a definition for the mixing rules from the excess Gibbs energy at infinite pressure. A detailed description of that model has been given by Solbraa (2002). The SRK-HV implementation used in this work has parameters regressed over a wide range of CO₂-water data, and the regression work is described in detail by Austegard et al. (2006). The SRK-HV evaluated in this work uses the Twu–Bluck–Cunningham (TBC) (Twu et al., 1991) formulation for computing the alpha parameter.

2.4. The corresponding states principle

The principle of corresponding states assumes that all substances exhibit the same behavior at a reduced state. A corresponding state EoS typically has one or more reference components described very accurately by a reference EoS. Therefore, the compressibility of the investigated fluids or mixtures can be evaluated as $Z = Z(V_{\text{Ref}}, T_{\text{Ref}}, \omega, \dots)$. In the corresponding states approach, the reference fluid volume V_{Ref} and temperature T_{Ref} are the reduced volume and temperature, V_{R} and T_{R} , of the fluid or the mixture investigated.

2.5. The extended corresponding states principle

2.5.1. Basic concept

In the extended corresponding states concept, the mapping between the investigated fluid or mixture T and V and the reference fluid V_{Ref} and T_{Ref} is done via the shape factors θ and ϕ . These shape factors take into account how the fluids or the mixture in consideration differ from the reference fluid, where $T_{\text{Ref}} = T/\theta$ and $V_{\text{Ref}} = V/\phi$. The shape factors θ and ϕ can be computed via shape factor functions, using semi-empirical functions, an accurate reference equation for each component, or using a simpler EoS. The work on shape factor functions started as early as 1968 by Leach et al. (1968). Subsequently, many contributions were made, examples are the work by Fisher and Leland (1970) and of Ely (1990), who has introduced the first exact shape factor concept. One of the most recent work on shape factor functions was conducted by Estela-Uribe and Trusler (1998). The computation of exact shape functions is computationally very expensive, which is why the concept was left behind and thought to be impractical for use with numerical simulations. However, several implementations of the concept of extended corresponding states use simpler equations of state to compute shape factors, which show a good compromise between accuracy and computation time.

2.5.2. The SPUNG EoS

The SPUNG EoS investigated here is an instance of the extended corresponding states approach, which was enlightened by the work of Mollerup (1980) and developed first for hydrocarbons. The SPUNG EoS uses the cubic SRK EoS to calculate the shape factors and propane as a reference fluid. Furthermore, it uses the accurate modified Benedict-Webb-Rubin (MBWR)

(Younglove and Ely, 1987) EoS for the reference fluid. The SPUNG EoS is described more in detail in the doctoral thesis by Jørstad (1993). It was developed for low temperature hydrocarbon mixtures, and it has improved density and enthalpy prediction while maintaining a good compromise in computational expenses. Propane was chosen as the reference fluid to ensure that the reduced temperature of the considered mixtures would always be above the reduced triple point of the reference fluid in order to avoid extrapolation of the reference equation. For CO₂ mixtures the choice of a different reference fluid and equation should be considered, but in this work only the original SPUNG EoS formulation was used.

3. Methodology

3.1. Numerical Tools

An in-house thermodynamic library was mainly used for the study presented. The library is a tool for predicting the thermodynamic properties using various approaches that ranges in level of sophistication and underlying theory. The SRK-HV model used here was the one described by Austegard et al. (2006) and with the regressed coefficients listed there. The library uses a tolerance of 10^{-4} for both the multi-phase flash algorithm and the compressibility factor calculations.

3.2. Setup of the investigation

3.2.1. Single phase density predictions, low to moderate pressures

The four EoSs were evaluated at a set of low to moderate pressures (up to 100 bars) that ensured a single phase at given temperatures and water

concentrations in the mixture. The pressures, levels of temperature and water concentrations were chosen to enable comparison with the experimental work of Patel and Eubank (1988). Four concentrations of 98, 90, 75 and 50% H₂O were evaluated. The concentration of 98% was evaluated at the temperatures of 225, 200, 100 and 50 °C. The 90% was evaluated at 200, 100 and 71 °C, the 75% was evaluated at 225, 200, and 100 °C, and finally the 50% was evaluated at 225, 200 and 125 °C. It was clear that, as the H₂O concentration increased in the mixture, it was not possible to go to some low temperatures while maintaining the mixture in gaseous phase conditions. This explains the differences in the lower bound of the evaluated temperatures at the four studied concentrations.

3.2.2. Single phase density predictions, high pressures

A more challenging set of conditions at elevated pressures over a wider range of concentrations was evaluated. The set of concentrations ranged from CO₂ dominant (90%) to H₂O dominant (90%). The pressures varied from 10 to 100 MPa. All experiments were conducted at a temperature of 400 °C. The evaluated conditions were chosen to enable comparisons with the experimental data of Seitz and Blencoe (1999).

3.2.3. Dew Line prediction

The dew lines were evaluated at five different concentrations of 2, 5, 10, 25 and 50% H₂O. The pressures were chosen to comply with the work done by Patel et al. (1987), and the dew temperatures were then computed dependently.

3.2.4. Rich phases density predictions

The EoSs were evaluated at four sets of data provided by King et al. (1992), Chiquet et al. (2007), Hebach et al. (2004) and the validated predictions by Bikkina et al. (2011). King et al. (1992) provided only water-rich liquid-phase densities between 6 to 24 MPa at three temperatures of 15, 20, and 25 °C co-existing with CO₂-rich liquid phase. The 15 and 25 °C test sets were chosen for the analysis here. Chiquet et al. (2007) provided densities of both water-rich and CO₂-rich phases when CO₂ were at supercritical conditions. The set of data covered pressures from 5 to 45 MPa, and the selected sets of temperatures were about 35, 50, 90 and 110 °C. The work done by Hebach et al. (2004) were used for comparisons of water-rich liquid phase densities co-existing with CO₂-rich gas phase. The selected cases were at temperatures of 19, 29, 39 and 49 °C and pressures less than 5 MPa to ensure a gaseous CO₂-rich phase. The results of Chiquet et al. (2007) and Hebach et al. (2004) were measured at temperatures slightly around the listed values, although precisely fixed for each point. The simulations conducted here uses the exact measurements temperature nodes. The group of Bikkina et al. (2011) provided validated predictions that cover the missing rich phases density of CO₂-rich liquid and the co-existing water-rich liquid densities and CO₂-rich gaseous phase. The selected Liquid Liquid Equilibrium (LLE) data of Bikkina et al. (2011) went over pressures between 8 to 21 MPa at one temperature of 25 °C. Finally, the Vapour Liquid Equilibrium (VLE) data went over pressures between 1 to 6 MPa at four temperatures of 25, 40, 50 and 60 °C.

3.2.5. Solubilities

The accuracy of the SPUNG and SRKs EoSs in predicting the mutual solubilities of CO₂ and H₂O was validated against experimental data. Pappa et al. (2009) reviewed the experimental data of CO₂-Water system solubilities and recommended six sets of mutual solubility experimental data for model regression and validations. The six sets are of Takenouchi and Kennedy (1964), Wiebe (1941), Bamberger et al. (2000), and Valtz et al. (2004), Mueller et al. (1988), and King et al. (1992). For this work we excluded King et al. (1992) and used the recent Hou et al. (2013) that cover the available intermediate pressures data at various temperatures and fill in some gaps. The latter work also validate the results against these the intermediate literature data sets and show very good fitting. The first study done by Takenouchi and Kennedy (1964) provided very high pressure solubilities ranging between 10 and 70 MPa at a temperature of 110 °C. The second study by Wiebe (1941) cover pressures between 1 to 70 MPa and temperatures between 25 and 100. However, we present only the results at 50 and 75 °C because mutual solubilities are only provided at these two temperatures. The study conducted by Bamberger et al. (2000) provided data over moderate pressures between 4 and 14 MPa at three temperatures of 50, 60 and 80 °C. The set of experimental data by Valtz et al. (2004) covered very low pressures at three temperatures of approximately 5, 25, and 45 °C. For the low temperature of 5 °C, the pressures ranged approximately between 0.5 and 1 MPa, the range went wider as the temperature increased reaching approximately the range of 0.1 to 7 MPa at the temperature of 45 °C. The last set of experimental data by Hou et al. (2013) cover a wide range of data for pressures around

1 to 17.5 MPa, and over temperature range of 25 to 175 °C. The last set by Mueller et al. (1988), provides solubility data at low pressures and high temperatures between 100 and 200 °C.

3.2.6. Sensitivity to the interaction parameter K_{ij}

The SPUNG EoS uses the SRK EoS for computing the shape factors and SRK EoS uses the symmetric interaction parameter K_{ij} for computing the mixing coefficients. Therefore, we performed a simple sensitivity study on the effects of tuning K_{ij} on the results. The tuning was done by matching the CO₂ solubilities as good as possible and letting the density and H₂O solubility be computed accordingly. The results of the tuning for the evaluated cases are plotted and labeled as *SPUNG-Reg K_{ij}* in the following.

3.2.7. Reference fluid sensitivity

An examination was conducted for the impact of using other reference fluids on the density predictions of the water-rich liquid phase. N₂, O₂, ethane (C1), methane (C2), iso-butane (IC4) and normal-butane (NC4) were used as a reference fluid for this study as an alternative to the originally used propane (C3). The aim of this part of the analysis was to find a criterion of selection or to search for the proper reference fluid to model CO₂-water mixtures.

3.3. Error definition

The errors of an EoS is measured here by the Relative Error (RE) and the Average of Absolute Deviation (AAD) defined for an arbitrary variable C as

$$RE(C_r, \%) = \frac{|C_{s,r} - C_{\text{exp},r}|}{C_{\text{exp},r}} \times 100 \quad (1)$$

and

$$AAD(C, \%) = \frac{100}{N} \times \sum_{r=1}^N \frac{|C_{s,r} - C_{\text{exp},r}|}{C_{\text{exp},r}} \quad (2)$$

Here, N is the total number of points, subscripts s and exp refer to simulation data and experimental data, respectively, and r is a point index.

4. Results

4.1. Single phase density, high pressures

The comparisons between the three EoSs for the high-pressure data sets of Seitz and Blencoe (1999) are plotted in Figs. 1 and 2. The former shows the density changes over pressures for various CO_2 content in the mixture, while the latter is an interesting re-plot of the data as density change over molar fraction of CO_2 for the various pressures.

[Figure 1 about here.]

[Figure 2 about here.]

4.2. Single phase density, low to moderate pressures

[Figure 3 about here.]

A comparison between the three EoSs for the low pressure data sets of Patel and Eubank (1988) are plotted in Fig. 3 for 2% H_2O and a temperature of 225 °C. Results for the three other temperatures of 50, 100 and 200 °C were virtually similar to those shown for 225 °C. Furthermore, the models

were compared to experimental data for the concentrations of 10% H₂O at temperatures 71, 100, 200 and 225 °C, for 25% H₂O at 100, 200 and 225 °C and for 50% H₂O at 125, 200 and 225 °C. For all these series of density variation with pressure, the errors were tiny and showed no significant dependency on temperature.

4.3. Dew line

The dew line predictions of SPUNG, SRK and SRK-HV are shown in Fig. 4 for three of the datasets from Patel et al. (1987). For another two datasets, 25% and 50% H₂O, the computed results matched the experimental data as good as for 10%, or better. At the compositions of 10% and 25% H₂O all the EoSs predicted pseudo critical pressures lower than the highest pressure of the experiments. Where, SRK-HV predicted 8.045, and 9.394 MPa pseudo critical pressures respectively, and SRK predicted 8.161, and 9.55 MPa respectively. Since SPUNG uses the SRK algorithm to calculate for the pseudo critical quantities, it predicted the same pseudo critical pressures as of SRK. Hence the highest pressure point of the 10% H₂O content from Patel et al. (1987) was not plotted. As seen, the results showed an improvement of the EoSs predictions as the water content increased.

[Figure 4 about here.]

4.4. Rich phases density prediction

4.4.1. CO₂-rich phases

The densities of the Supercritical Liquid Equilibrium (SGLE) of the CO₂-rich phase co-existing with a liquid water-rich phase were modeled, and the results are presented in comparison with the experimental data of

Chiquet et al. (2007) in Fig. 5. The AAD of the supercritical CO₂-rich phase density predictions are presented in Table 1.

From Fig. 5, two experimental points seemed to be anomalous: at 110 °C, 25 MPa and 90 °C, 7 MPa. These points deviated from the trend of each dataset, and the model errors jumped significantly. For the discussion, the AADs were recalculated without these two points in Table 1.

Model computations of the liquid CO₂-rich phase were compared with the predicted data of Bikkina et al. (2011) in Fig. 6. The corresponding AADs are included in Table 1.

For the gaseous CO₂-rich phase predictions, errors compared with the data of Bikkina et al. (2011) were very small with all models and very similar to the single gas phase results.

However, the values of the binary interaction parameter K_{ij} used to get the proper CO₂ solubility decreased with increasing temperature. The used values were -1.44 , -0.130 , -0.115 and -0.107 , respectively, for 25, 40, 50 and 60 °C. The AADs for the entire used dataset are included in Table 1. For gaseous phase, the AADs reported were temperature averaged.

[Figure 5 about here.]

[Figure 6 about here.]

[Table 1 about here.]

4.4.2. *Water rich liquid density prediction*

The density predictions of the liquid water-rich phase co-existing with a supercritical CO₂-rich phase at a temperature of 35 °C are presented in

comparison with the experimental data of Chiquet et al. (2007) in Fig. 7. The results for the temperatures of 50, 90 and 110 °C were very similar in trend. However, the K_{ij} values used to get the proper CO₂ solubility decreased with temperature increase, where the used values were -0.132 , -0.118 , -0.068 , -0.045 , respectively, for the temperatures from 35 to 110 °C.

The results of the density predictions of the liquid water-rich phase co-existing with liquid CO₂-rich phase at a temperature of 25 °C are plotted in Fig. 8. The results of 15 °C behaved very similar to those at 25 °C and are not shown. The used K_{ij} values were -0.15 and -0.14 , respectively.

[Figure 7 about here.]

[Figure 8 about here.]

Density predictions of the liquid water-rich phase co-existing with gaseous CO₂-rich phase at a temperature of 29 °C are plotted in Fig. 9. The results of 19, 39 and 49 °C were very similar. The used K_{ij} values were -0.154 , -0.141 , -0.129 and -0.118 , respectively.

Table 2 contains a summary of the results in terms of temperature averaged AADs.

[Table 2 about here.]

[Figure 9 about here.]

As mentioned in Sect. 2.5.2, propane was chosen as the reference fluid in the SPUNG EoS.

Table 3 shows the results from the reference fluid sensitivity study. The AADs averaged over temperature.

The C3 (propane) results are the same as shown for SPUNG in Fig. 9. Only one temperature out of the evaluated four was presented due to similarity in trends and uniformity of the errors.

[Table 3 about here.]

4.5. Solubilities

The behavior of SPUNG, SRK and SRK-HV at low pressures-low temperatures were evaluated and results in comparison to the work conducted by Valtz et al. (2004) are plotted in Fig. 10. The solubilities at 25.13 °C were also evaluated towards experimental data with results comparable to those shown. The AADs are presented in Table 4.

[Figure 10 about here.]

[Table 4 about here.]

The behavior of SPUNG, SRK and SRK-HV at low pressures-high temperatures were evaluated and results in comparison to the work conducted by Mueller et al. (1988) are plotted in Fig. 11. The results of the intermediate temperatures were not plotted as the trend is obvious that the error drops with temperature increase. The AADs at 100, 140 and 200 °C are presented in Table 5.

[Figure 11 about here.]

[Table 5 about here.]

The solubility over moderate pressures were predicted by the three models at temperatures of 50, 60 and 80 °C, which were chosen in consistency to the experimental work of Bamberger et al. (2000). Results are plotted in Figs. 12 and 13. The CO₂ solubility results at 50 and 60 °C turned out very similar to those shown at 80 °C. For H₂O the 50 °C results were similar to those shown for 60 °C (Fig. 13), with some better match with experimental data for SRK-HV. The AADs are presented in Table 6. A K_{ij} sensitivity study was conducted over this set of conditions. The results showed that any improvement of CO₂ solubilities prediction causes a significant increase in the H₂O solubility prediction errors for using SRK, and SPUNG EoS.

[Figure 12 about here.]

[Figure 13 about here.]

[Table 6 about here.]

The results of the comparisons to Hou et al. (2013) are plotted in Fig. ???. The plot is only at the lowest and highest temperatures since the trend is the same that as the temperature increases the errors drop.

The summery of AADs over temperature is plotted in Fig. ???.

[Figure 14 about here.]

The comparison with Wiebe (1941) is presented in Table 7. There were no compromise tuning K_{ij} and a trade-off arises.

[Table 7 about here.]

The evaluated EoSs were used to predict the mutual solubilities of CO₂ and H₂O in the binary polar mixture of CO₂-water at very high pressures. The conditions were chosen in compliance with the work of Takenouchi and Kennedy (1964). Pressures from around 10 to 70 MPa were used for prediction at a temperature of 110 °C. The results are plotted in a comparison with experimental data in Fig. 15. The errors are described in terms of AADs and presented in Table 8.

[Figure 15 about here.]

[Table 8 about here.]

5. Discussion

5.1. Single phase and dew line prediction

Regarding dew line predictions or saturation conditions, Fig. 4 and results for higher H₂O content showed that all the three EoSs were behaving well in computing the saturation line. An exception is the case of 2% H₂O, which seems to be challenging for all the models. The simulations also showed that all the tested models predicted a low pseudo-critical pressure for the cases of 10% and 25% H₂O.

For low-pressure density calculations presented in Fig. 3, the densities comparison showed that the errors over the investigated intervals were on average very small for all the tested EoSs. Nevertheless, looking closely at the errors behavior, it was observed that the errors increased as the pressure increased and the mixture gradually departed from ideal behavior. The important observation was that the errors of SRK and SRK-HV grew steeply

compared to that of the SPUNG EoS as the pressure went above a certain threshold in most of the cases. This behavior resulted in REs of SRK and SRK-HV that were multiples of that of SPUNG at the upper bound of the tested (pressure and H₂O) intervals.

From the results of the high-pressure single-phase density calculations Figs. 1 and 2, except for GERG, the comparisons showed an increase of the errors as the pressure increased and as the H₂O content increased. While at low pressure the increase and the relative errors value were small, the errors jumped to an order of magnitude higher at the combination of the upper-bounds of both intervals.

The figures also show clearly that the errors behavior of SPUNG is much better than that of SRK and SRK-HV and, considering the computational expenses study by Wilhelmssen et al. (2012), it can be concluded that it is a good compromise between sophisticated and the cubic EoSs.

In fact, there are some sets of conditions where the SPUNG EoS even performed better than GERG. These sets are readily observed in Fig. 2, where GERG was tuned very well at the H₂O or CO₂ dominant conditions, but got worse as the mole fraction moved towards the 50% value.

Although the errors of SPUNG reached 20% at the extreme of the investigated conditions, the method has a possible high potential for improvement via using other reference fluids, while the SRKs do not have the same potential. Further research can evaluate this potential.

The inaccuracies of the used cubic EoSs are due to the simple structure of the models, which have very few parameters to tune. A study similar to the presented work but for other mixtures was made by Li and Yan (2009),

who reported the same inaccuracies using SRK and other cubic equations for mixtures of CH₄, H₂S, N₂ and Ar. Furthermore, Li et al. (2011) reviewed several studies testing cubic equations for gas and liquid density predictions for other mixtures. In our investigation, the errors reached approximately 25% at the extreme conditions using cubic EoSs. This was higher than in the studies of other mixtures, emphasizing how challenging this particular mixture is for cubic EoSs compared to the other mixtures. In addition, this showed the need for a more predictive concept when dealing with CO₂-water mixture.

On the other hand, the SPUNG EoS superiority in density computations was inherited from the use of the 32-parameter MBWR reference equation, which is very accurate for propane. However, the errors of the SPUNG EoS came from the incapability of propane to achieve the high density of the CO₂ - water liquid phase.

5.2. Rich phases density prediction

5.2.1. CO₂-rich gas phase

The results of CO₂-rich gas phase show clearly that the accuracy of all the evaluated EoSs was very good. A high accuracy for gas phase density using cubic EoSs was reported in many studies that were listed in the review article of Li et al. (2011). Furthermore, the solubility of the H₂O into CO₂-rich gas phase was too small to cause a challenge in modelling, as reported by Hebach et al. (2004).

5.2.2. CO₂-rich liquid phase

The results in Fig. 6 show that at the low pressure side, the errors of the SRKs were around 12% compared to 4% of SPUNG EoS. As the pressure went higher, the errors of all the EoSs became lower. However, the errors of SPUNG dropped to around 0.17 while the SRKs errors remained high at approximately 8%. This behavior was not revealed by the AADs in Table 1, which average the REs over the predicted interval to approximately 2% of SPUNG and 9% for SRKs.

5.2.3. CO₂-rich supercritical phase

As noted in Sect. 4.4.1, two measurement points, (7 MPa, about 90 °C) and (25 MPa, about 110 °C), in Fig. 5 seemed to be anomalous. The deviation is seen for all the three evaluated models. Since the models are based on different theories, the anomaly suggested a measurement error. Alternatively, there might be a feature that is not captured by any of the models. At the two low evaluated temperatures, the predictions of SPUNG EoS were substantially better than those of the SRKs, especially in capturing the steep change in density over the pressures between 5 and 10 MPa at about 35 °C and between 5 and 15 MPa at about 50 °C, as observed in Fig. 5. In these two cases, the errors of SRKs jumped to around 15 and 13%, while the SPUNG errors were below 1.3%. Furthermore, the errors of the SRKs were reduced gradually as the density to pressure curve started saturating, while the errors of SPUNG remained low over the entire interval. Table 1 flattened out this behavior to AADs, which in their turns showed the high accuracy of SPUNG EoS prediction compared to SRKs EoSs. At the two evaluated high temperatures, the two mentioned points gave exceptional peaks in the error.

Apart from this, the errors were similar to those of the lower temperatures, although the amplitude was much lower, and the RE distribution in general had a more flattened profile as the density increase with pressure was much more gradual at high temperatures than at the low temperature cases. The behavior of SPUNG remained superior, which can also be observed in the results summarized in terms of AADs in Table 1.

5.2.4. *Water-rich liquid phase*

The results in Fig. 7 and the results for other temperatures (not presented) showed that the errors of all the evaluated EoSs were considerable especially when compared to the results of Tsivintzelis et al. (2011), Diamantonis and Economou (2012). The errors were not very sensitive to temperature and pressure. This caused the REs to be rather flat and made the AAD a very representative measure.

The capture of the temperature dependency was good. Furthermore, the insensitivity to both the pressure and co-existing phase was virtual as it was due to the incapability of all the EoSs to capture the high liquid-water density. This is regardless of how well the models capture the CO₂ solubility effect due to the increase in pressure. However, looking carefully to the SRK-HV slope in density-pressure behavior and the rather horizontal REs compared to the other evaluated EoSs, it could be observed that only SRK-HV captured the effect of CO₂ solubility as a function of pressure properly due to the superior prediction of CO₂ solubility using SRK-HV, which will be discussed below. This observation was supported by comparing the predictions of pure water at the same pressures and the one with CO₂ solubility, where SPUNG and SRK showed almost no difference in density predictions, whereas SRK-HV

predicted the density difference accurately. This observation was not very clear from the first glance at the graphs, since the difference it made to capture the CO₂ solubility properly was of 1.5%, while the errors were above 20% for all the evaluated EoSs. Although SRK-HV predicted the deviation part correctly, SPUNG density prediction was superior to both SRKs, with a potential of improvement by using other reference fluids.

This discussion applies to the results of water-rich liquid phase co-existing with liquid and gaseous CO₂-rich phases in Figs. 8-9. Nevertheless, the difference in the case of water-rich liquid co-existing with gaseous CO₂-rich phase was that the measured density had a slight increase in with increased pressure, Fig. 9. This is due to the interfacial tension as reported by Hebach et al. (2004). The solubility was captured very good by SRK-HV. This can be observed in the inclination of the SRK-HV curve, which has the very similar slope as of the experimental data in the density results of Fig. 9.

An observation from Fig. 7 was that the point of 7 MPa seemed to deviate from the trend of the remaining points. Unless this was just an inaccuracy, the phenomenon was not captured by the models.

5.3. Solubilities

The results in Fig. 15 and Table 8 show that the predictability of SRK-HV for the solubility of CO₂ in water was much better than those of SRK and SPUNG EoSs and of low errors. The predictions by SPUNG and SRK were poor. On the other hand, the prediction of the H₂O solubility by SRK-HV was much worse than that of SRK and SPUNG, where all the models were inaccurate. Since SRK uses a symmetric interaction parameter K_{ij} between CO₂ and H₂O in the van der Waals geometric mean-based mixing rules, it

was expected that the SRK predictability of one of the mutual solubilities will be that low due to the polar nature of the mixture. The results suggested that SPUNG EoS inherits this impotence from SRK since it uses SRK to compute the shape factors.

The comparison with Wiebe (1941) at high pressures and low temperatures shows very low predictability of all the EoSs with fare wrong results using SPUNG and SRK EoSs. There were no possibility for improvement for SPUNG and SRK EoSs by regression.

The solubility at moderate pressures, chosen in consistency to the experimental work conducted by Bamberger et al. (2000), were predicted by the three models. The results in Figs. 12 and 13 and AADs in Table 6, show that the errors in predicting CO₂ solubility became more severe than those at very high pressures for SPUNG and SRK EoSs. This highlighted the superior behavior of SRK-HV even more. Furthermore, the errors of SPUNG and SRK were reduced as the temperature increased, which suggested a need for correlating the interaction parameter K_{ij} to temperature in addition to a more general mixing rule. This analysis was confirmed by the K_{ij} sensitivity study conducted here (see Sect. 5.4). The predictability of SPUNG and SRK improved for H₂O solubilities, while that of SRK-HV improved for both mutual solubilities and behaved much better than those of SPUNG and SRK.

The comparison to the set of data of Hou et al. (2013) shows the same behavior as of the one with Bamberger et al. (2000) at similar temperatures. However, that the errors of all the EoSs reduced significantly as the temperature increased.

For low pressures, the results in Fig. 10 and the AADs in Table 4, showed the same trend in comparison with the experimental data of Bamberger et al. (2000), except that SRK-HV did not behave equally well.

For the low pressures high temperatures in Fig. 11 the results show good and improving predictability as temperature increases.

In general, the predictions of all the EoSs improves with temperatures increase at all pressures.

In general the predictions of solubility improves as the temperature increases by all the EoSs.

5.4. Effects of the interaction parameter K_{ij}

Since the impotence of SPUNG in predicting the solubilities of CO₂ - water was thought to be inherited from SRK due to the use of the symmetric interaction parameter K_{ij} , a simple sensitivity study on the effects of tuning K_{ij} was conducted as explained in Sec. 3.2.6. The results of the tuning for the evaluated very high and low-pressure cases are plotted in Figs. 15, 11 and 10. The AADs are presented in Tables 8, 5 and 4. These results showed that at these conditions there existed a K_{ij} that could improve the mutual solubilities together, and that compromised the errors better than SRK-HV for the very high pressure, and for the low pressures-high temperatures cases. This implies a potential improvement by regression. Unfortunately, this behavior did not hold for the moderate pressures, and high pressures low temperatures cases. There, the CO₂ solubility errors could be improved, but causing the errors of H₂O solubility to jump high with the expected counter effects due to the use of the geometric mean mixing rules. This behavior shows clearly that SPUNG EoS solubility prediction is limited to that of the EoS used to

compute the shape factors.

The tuning of K_{ij} influence the rich-phase density predictions mainly through solubility. This is because K_{ij} influence mainly the energy parameter a , and the co-volume parameter b in the cubic EoSs formulations. In order to give a sense of the impact of each of the mutual solubility on the density predictions for CO₂-water system, a study was conducted at the conditions used for the density analysis discussed here. Since Chiquet et al. (2007), Hebach et al. (2004) and Bikkina et al. (2011) have not provided solubilities, the tuning was done by matching SRK-HV CO₂ solubility as good as possible. This was thought to be a valid step because SRK-HV showed a significantly good prediction of CO₂ solubility at similar pressure ranges in the work of Austegard et al. (2006). In addition, the comparison here, Figs. 12 - 13 and Table 6, supported the same claim. The density predictions of the K_{ij} tuned SPUNG EoS are included in the figures and summarized in the tables of the density predictions study. The results show minor improvement on H₂O-rich phase density and major dis-improvement on CO₂-rich phase density due to the conjugate dis-improvement in H₂O solubility prediction that is induced from the mixing rule.

It is important also to highlight the observation that the tuning showed a temperature-dependent behavior for K_{ij} that was almost insensitive to the pressure and co-existing phases.

Since the solubilities are important for deciding co-existing phases, especially for small impurities of H₂O in CO₂ or vice versa, and since SPUNG EoS has shown high potential, we are motivated under the guidance of this work for further developing the method to overcome this weakness. A more

elaborated mixing rule that shall take into account the polar nature of the system, as well as the temperature dependency shown in this work, is needed.

5.5. Reference fluid sensitivity

The results in Fig. ?? showed clearly that the choice of reference fluid had a significant impact on the properties predictions and, in particular, on density predictions. Furthermore, the trend observed in the results was very interesting, where a heavier reference fluid within the set of hydrocarbons gave better predictions of the density compared to a lighter. Also within the set of O₂ and N₂ the same trend was seen. For all the reference fluids in Fig. ??, the curves of the REs showed almost equal slopes, which implied a low impact on solubility predictions.

6. Conclusions

The three tested EoSs predicted the dew temperature with high quality and precision, but predicted low pseudo critical pressure for two tested sets.

For single phase, at low pressure gas phase, SPUNG EoS exhibits a better behavior to SRK- and SRK-HV cubic EoSs. However, the REs are low for all models. The role of SPUNG become significant as high pressures are of concern, where the error become considerable.

SPUNG has a superior behavior in predicting the rich phases density of the CO₂-water system compared to the evaluated cubic EoSs. Although CO₂ solubility prediction of SPUNG is very low at moderate pressures and low temperatures, the impact on density calculations for the H₂O-rich phase is not pronounceable. Improving the CO₂ solubility on the benefits of that of H₂O, lead to severe mis-prediction in the density of the CO₂-rich phase. The

impact on the over all density prediction of the system will depend on the feed composition. Therefore, for the cases where water is an impurity the impact of CO₂ solubility mis-prediction will have much less impact on the over all density prediction.

The effect of varying the reference fluids was investigated, and the errors span between the lightest and the heaviest reference fluid was large. This implies a significant impact of the reference fluid on the properties prediction. Nevertheless, the heaviest evaluated hydrocarbon was not heavy enough to give a significant improvement. However, the observed trend and highlighted criterion of the search for a reference fluid rises the expectations in the SPUNG EoS potential for improving the water-rich phase density prediction, if a proper reference fluid is found, while the cubic EoSs don't have a similar potential.

SRK-HV EoS predicted the mutual solubilities for the binary polar mixture with high accuracy. Nevertheless, it showed much poorer predictability of the density of the CO₂-water system in general and compared to SPUNG in particular.

SRK EoS with van der Waals mixing rules combines the impotence of both SPUNG and SRK-HV EoS. Therefore, it is not recommend for this system, unless low-pressure gas-phase densities are the only interest.

The study show that SPUNG EoS solubility predictability is limited by the EoS used for the computation of the shape factors, here, is limited by SRK. However the predictability of the density is controlled independently by the reference fluid and the reference equation used. As one of the powerful

features of the concept is to allow a free choice of the EoS for the shape factors, the reference fluid, and the reference equation (given that the reference fluid coefficients exist for this reference equation), a promising option is to use an Asymmetric quadratic mixing rule. It is also possible to use SRK-HV, which showed a very high success for solubility predictions of CO₂-water system.

Acknowledgement: This work was financed through the CO₂ Dynamics project. The authors acknowledge the support from the Research Council of Norway (189978), Gassco AS, Statoil Petroleum AS and Vattenfall AB.

References

- Austegard, A., Solbraa, E., de Koeijer, G., Mølnvik, M.J., 2006. Thermodynamic models for calculating mutual solubilities in H₂O-CO₂-CH₄ mixtures. *Chem. Eng. Res. Des.*, 84(9), 781 – 794.
- Bamberger, A., Sieder, G., Maurer, G., 2000. High-pressure (vapor+liquid) equilibrium in binary mixtures of (carbon dioxide+water or acetic acid) at temperatures from 313 to 353 K. *J. Supercrit. Fluids*, 17(2), 97 – 110.
- Bikkina, P.K., Shoham, O., Uppaluri, R., 2011. Equilibrated interfacial tension data of the CO₂-water system at high pressures and moderate temperatures. *J. Chem. Eng. Data*, 56(10), 3725–3733.
- Chapman, W.G., Gubbins, K.E., Jackson, G., Radosz, M., 1990. New refer-

- ence equation of state for associating liquids. *Ind. Eng. Chem. Res.*, 29(8), 1709–1721.
- Chiquet, P., Daridon, J.L., Broseta, D., Thibeau, S., 2007. CO₂/water interfacial tensions under pressure and temperature conditions of CO₂ geological storage. *Energy Convers. Manage.*, 48(3), 736 – 744.
- Diamantonis, N.I., Economou, I.G., 2012. Modeling the phase equilibria of a H₂O-CO₂ mixture with pc-saft and tpc-psaft equations of state. *Mol. Phys.*, 110(11-12), 1205–1212.
- Ely, J.F., 1990. A predictive, exact shape factor extended corresponding states model for mixtures. *Adv. Cryog. Eng.*, 35, 1511–1520.
- Estela-Uribe, J.F., Trusler, J.P.M., 1998. Shape factors for the light hydrocarbons. *Fluid Phase Equilib.*, 150-151, 225 – 234.
- Fisher, G.D., Leland, T.W., 1970. Corresponding states principle using shape factors. *Ind. Eng. Chem. Fundam.*, 9(4), 537–544.
- Hebach, A., Oberhof, A., Dahmen, N., 2004. Density of water + carbon dioxide at elevated pressures: measurements and correlation. *J. Chem. Eng. Data*, 49(4), 950–953.
- Hendriks, E., Kontogeorgis, G.M., Dohrn, R., de Hemptinne, J.C., Economou, I.G., Zilnik, L.F., Vesovic, V., 2010. Industrial requirements for thermodynamics and transport properties. *Ind. Eng. Chem. Res.*, 49(22), 11131–11141.

- Hou, S.X., Maitland, G.C., Trusler, J.M., 2013. Measurement and modeling of the phase behavior of the (carbon dioxide + water) mixture at temperatures from 298.15 k to 448.15 k. *J. Supercrit. Fluids*, 73, 87–96.
- Huron, M.J., Vidal, J., 1979. New mixing rules in simple equations of state for representing vapour-liquid equilibria of strongly non-ideal mixtures. *Fluid Phase Equilib.*, 3(4), 255 – 271.
- Ibrahim, M., Skaugen, G., Ertesvåg, I.S., 2012. Preliminary evaluation of the {SPUNG} equation of state for modelling the thermodynamic properties of co₂-water mixtures. *Energy Procedia*, 26, 90 – 97.
- Jørstad, O., 1993. Equations of state for hydrocarbon mixtures. Dr. Ing. thesis No. NTH 1993:92. Norwegian Institute of Technology, Trondheim, Norway.
- King, M.B., Mubarak, A., Kim, J.D., Bott, T.R., 1992. The mutual solubilities of water with supercritical and liquid carbon dioxides. *J. Supercrit. Fluids*, 5(4), 296 – 302.
- Kontogeorgis, G.M., Voutsas, E.C., Yakoumis, I.V., Tassios, D.P., 1996. An equation of state for associating fluids. *Ind. Eng. Chem. Res.*, 35(11), 4310–4318.
- Kunz, O., Klimeck, R., Wagner, W., Jaeschke, M., 2007. The GERG-2004 Wide-Range Equation of State for Natural Gases and Other Mixtures. GERG TM15, VDI Verlag, Düsseldorf, Germany.
- Leach, J.W., Chappellear, P.S., Leland, T.W., 1968. Use of molecular shape

- factors in vapor-liquid equilibrium calculations with the corresponding states principle. *AIChE J.*, 14(4), 568–576.
- Lemmon, E.W., Huber, M.L., McLinden, M.O., 2010. NIST Standard Reference Database 23: Reference Fluid Thermodynamic and Transport Properties - REFPROP, version 9.0. National Institute of Standards and Technology, Standard Reference Data Program, Gaithersburg, Maryland.
- Li, H., Jakobsen, J.P., Wilhelmsen, Ø., Yan, J., 2011. PVTxy properties of CO₂ mixtures relevant for CO₂ capture, transport and storage: Review of available experimental data and theoretical models. *Appl. Energy*, 88(11), 3567 – 3579.
- Li, H., Yan, J., 2009. Impacts of equations of state (EOS) and impurities on the volume calculation of CO₂ mixtures in the applications of CO₂ capture and storage (CCS) processes. *Appl. Energy*, 86(12), 2760 – 2770.
- Mollerup, J., 1980. Thermodynamic properties from corresponding states theory. *Fluid Phase Equilib.*, 4(1-2), 11 – 34.
- Mueller, G., Bender, E., Maurer, G., 1988. Das dampf-fluessigkeitsgleichgewicht des ternaeren systems ammoniak-kohlendioxid-wasser bei hohn wassergehalten im bereich zwischen 373 und 473 kelvin. *Ber. Bunsenges. Phys. Chem.*, 92, 148–160.
- Pappa, G.D., Perakis, C., Tsimpanogiannis, I.N., Voutsas, E.C., 2009. Thermodynamic modeling of the vaporliquid equilibrium of the co₂/h₂o mixtures. *Fluid Phase Equilib.*, 284(1), 56–63.

- Patel, M.R., Eubank, P.T., 1988. Experimental densities and derived thermodynamic properties for carbon dioxide-water mixtures. *J. Chem. Eng. Data*, 33(2), 185–193.
- Patel, M.R., Holste, J.C., Hall, K.R., Eubank, P.T., 1987. Thermophysical properties of gaseous carbon dioxide-water mixtures. *Fluid Phase Equilib.*, 36, 279 – 299.
- Peng, D.Y., Robinson, D.B., 1976. A new two-constant equation of state. *Ind. Eng. Chem. Fundam.*, 15(1), 59–64.
- Seitz, J.C., Blencoe, J.G., 1999. The CO₂-H₂O system. I. Experimental determination of volumetric properties at 400°C, 10-100 MPa. *Geochim. Cosmochim. Acta*, 63(10), 1559 – 1569.
- Soave, G., 1972. Equilibrium constants from a modified Redlich-Kwong equation of state. *Chem. Eng. Sci.*, 27(6), 1197 – 1203.
- Solbraa, E., 2002. Equilibrium and non-equilibrium thermodynamics of natural gas processing. Dr. Ing. thesis No. 2002:146. Norwegian University of Science and Technol., Trondheim, Norway.
- Span, R., Wagner, W., 1996. A new equation of state for carbon dioxide covering the fluid region from the tripple-point temperature to 1100 K at pressures up to 800 MPa. *J. Phys. Chem. Ref. Data*, 25(6), 1509–1596.
- Takenouchi, S., Kennedy, G.C., 1964. The binary system H₂O-CO₂ at high temperatures and pressures. *Am. J. Sci.*, 262(9), 1055–1074.

- Tsivintzelis, I., Kontogeorgis, G.M., Michelsen, M.L., Stenby, E.H., 2011. Modeling phase equilibria for acid gas mixtures using the cpa equation of state. part ii: Binary mixtures with CO₂. *Fluid Phase Equilib.*, 306(1), 3856.
- Twu, C.H., Bluck, D., Cunningham, J.R., Coon, J.E., 1991. A cubic equation of state with a new alpha function and a new mixing rule. *Fluid Phase Equilib.*, 69, 33 – 50.
- Valtz, A., Chapoy, A., Coquelet, C., Paricaud, P., Richon, D., 2004. Vapour-liquid equilibria in the carbon dioxide-water system, measurement and modelling from 278.2 to 318.2 K. *Fluid Phase Equilib.*, 226, 333 – 344.
- Wiebe, R., 1941. The binary system carbon dioxide-water under pressure. *J. Am. Chem. Soc.*, 29(3), 475–481.
- Wilhelmsen, Ø., Skaugen, G., Jørstad, O., Li, H., 2012. Evaluation of SPUNG and other equations of state for use in carbon capture and storage modelling. *Energy Procedia*, 23, 236 – 245.
- Younglove, B.A., Ely, J.F., 1987. Thermophysical properties of fluids: II. Methane, ethane, propane, isobutane, and normal butane. *J. Phys. Chem. Ref. Data*, 16(4), 577–798.

List of figures caption:

Figure 1. Density computations in comparison with experimental data of Seitz and Blencoe (1999), over pressures up to 100 MPa at 90% and 10% CO₂ and a temperature of 400 °C.

Figure 2. Density computations in comparison with experimental data of Seitz and Blencoe (1999), over mole fractions of CO₂ at different pressures and a temperature of 400 °C.

Figure 3. Gas phase density calculations in comparison with experimental data of Patel and Eubank (1988) at 2% H₂O and a temperature of 225 °C.

Figure 4. Dew line temperature predictions in comparison with experimental data of Patel et al. (1987).

Figure 5. SGLE CO₂-rich phase density predictions at temperatures about 35, 50, 90 and 110 °C in comparison with Chiquet et al. (2007) experimental data.

Figure 6. LLE CO₂-rich phase densities prediction at a temperature of 25 °C in comparison to predictions of Bikkina et al. (2011).

Figure 7. Densities of the liquid water-rich phase co-existing with a supercritical CO₂-rich phase at a temperature about 35 °C in comparison with Chiquet et al. (2007) experimental data.

Figure 8. LLE water-rich phase density predictions at a temperature 25 °C in comparison with King et al. (1992) experimental data.

Figure 9. Densities of the liquid water-rich phase co-existing with a gaseous CO₂-rich phase at a temperature about 29 °C in comparison with Hebach et al. (2004) experimental data.

Figure 10. CO₂ and H₂O solubilities over low pressures and at temperatures of 5 and 45 °C in comparison with Valtz et al. (2004) experimental data.

Figure 11. CO₂ and H₂O solubilities over low pressures and at temperatures of 100 and 200 °C in comparison with Mueller et al. (1988) experimental data.

Figure 12. CO₂ solubilities over moderate pressures and at a temperature of

80 °C in comparison with Bamberger et al. (2000) experimental data.

Figure 13. H₂O solubilities over moderate pressures and at temperatures of 60 and 80 °C in comparison with Bamberger et al. (2000) experimental data.

Figure 14. CO₂ and H₂O solubilities computations in comparison with experimental data of Hou et al. (2013)

Figure 15. CO₂ and H₂O solubilities over very high pressures and a temperature of 110 °C in comparison with Takenouchi and Kennedy (1964) experimental data.

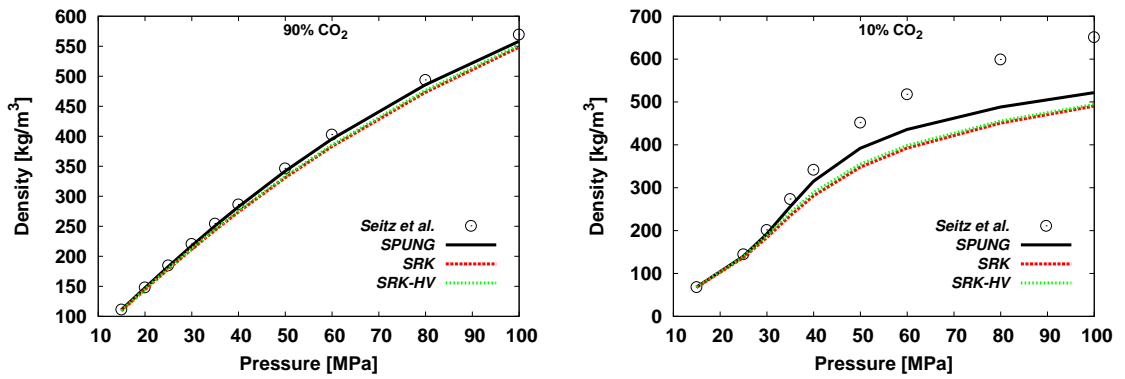


Figure 1: Density computations in comparison with experimental data of Seitz and Blencoe (1999), over pressures up to 100 MPa at 90% and 10% CO₂ and a temperature of 400 °C

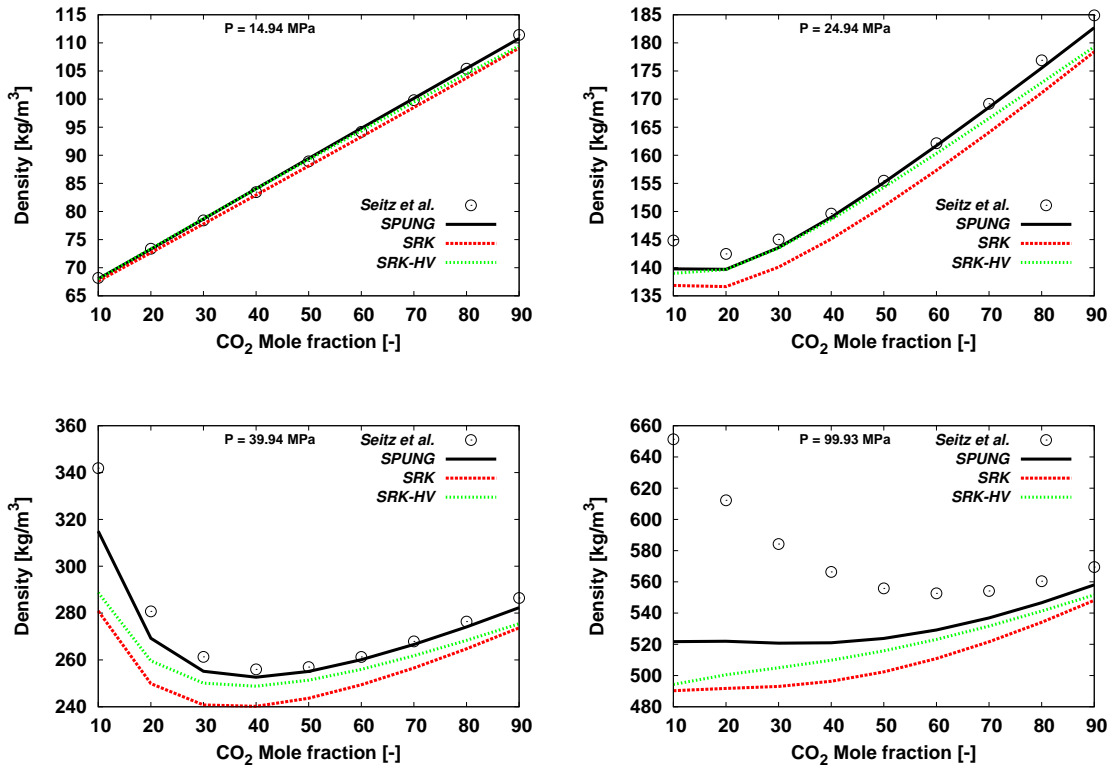


Figure 2: Density computations in comparison with experimental data of Seitz and Blencoe (1999), over mole fractions of CO₂ at different pressures and a temperature of 400 °C

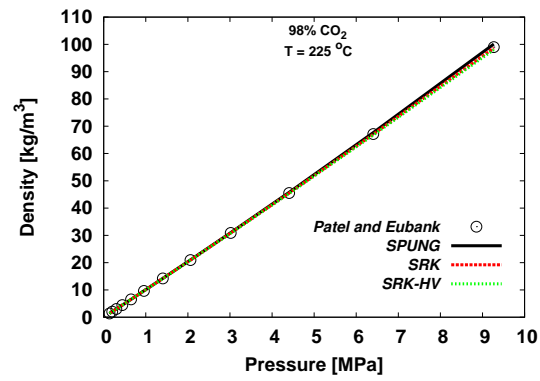


Figure 3: Gas phase density calculations in comparison with experimental data of Patel and Eubank (1988) at 2% H₂O and a temperature of 225 °C

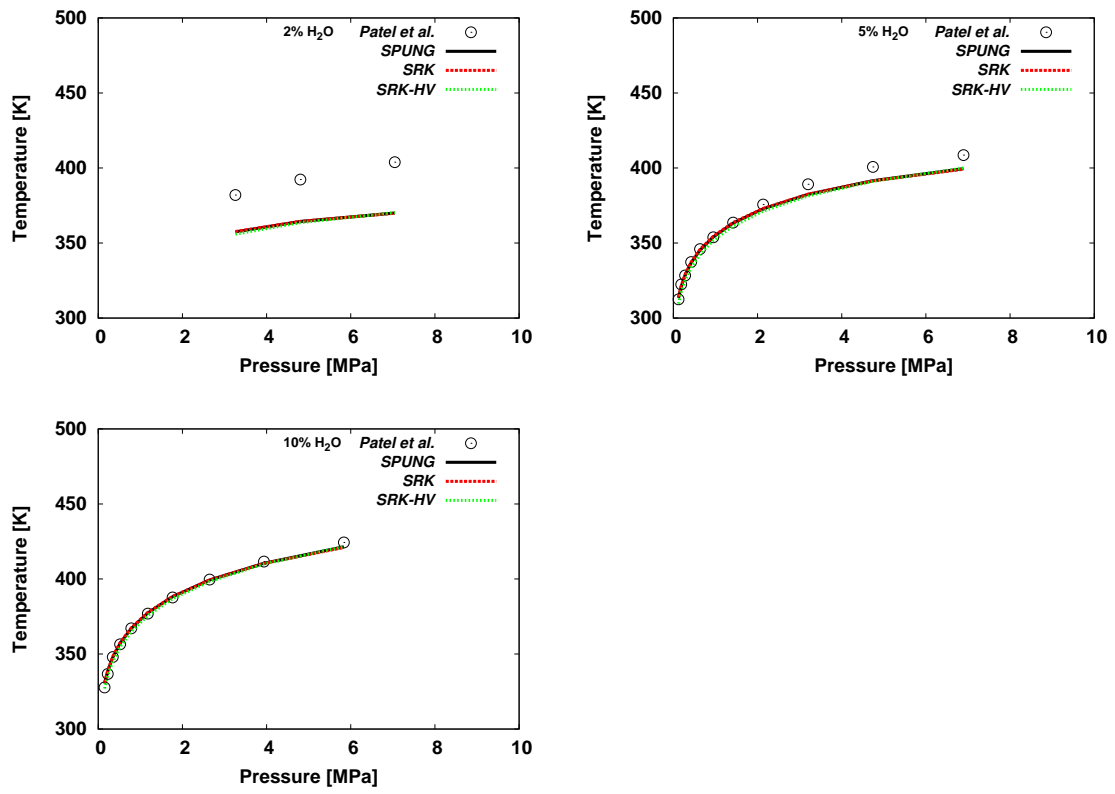


Figure 4: Dew line temperature predictions in comparison with experimental data of Patel et al. (1987)

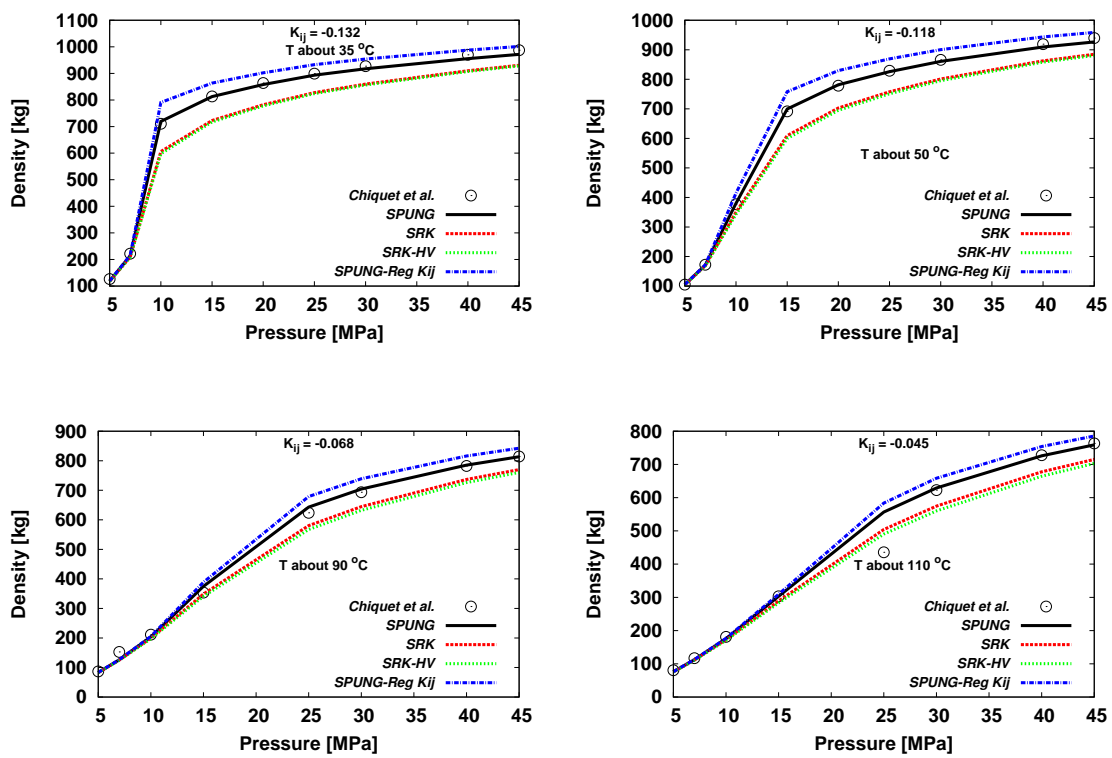


Figure 5: SGLE CO₂-rich phase density predictions at temperatures about 35, 50, 90 and 110 °C in comparison with Chiquet et al. (2007) experimental data

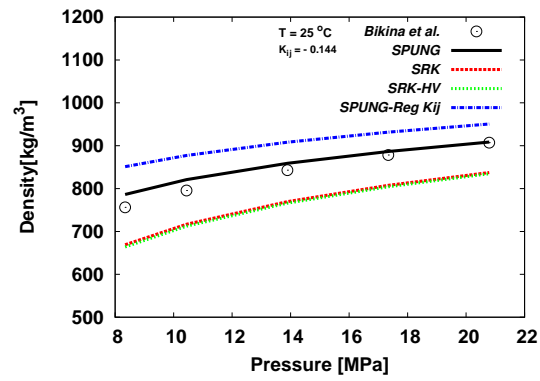


Figure 6: LLE CO₂-rich phase densities prediction at a temperature of 25 °C in comparison to predictions of Bikina et al. (2011)

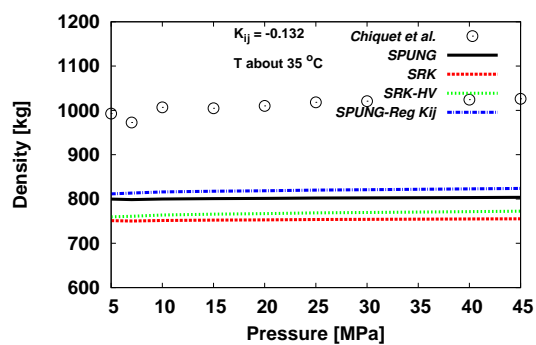


Figure 7: Densities of the liquid water-rich phase co-existing with a supercritical CO₂-rich phase at a temperature about 35 °C in comparison with Chiquet et al. (2007) experimental data

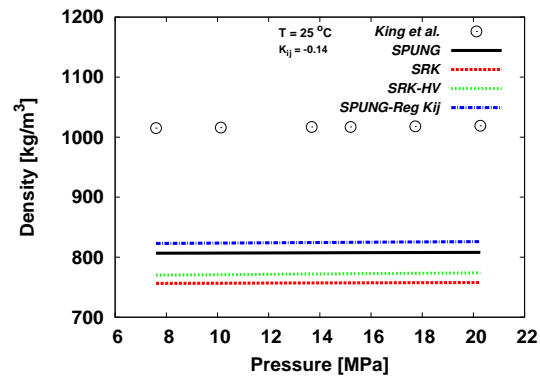


Figure 8: LLE water-rich phase density predictions at a temperature $25\text{ }^{\circ}\text{C}$ in comparison with King et al. (1992) experimental data

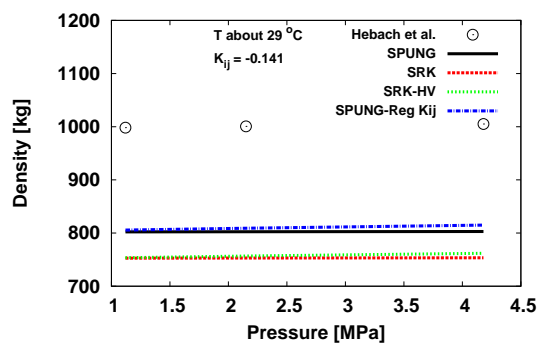


Figure 9: Densities of the liquid water-rich phase co-existing with a gaseous CO₂-rich phase at a temperature about 29°C in comparison with Hebach et al. (2004) experimental data

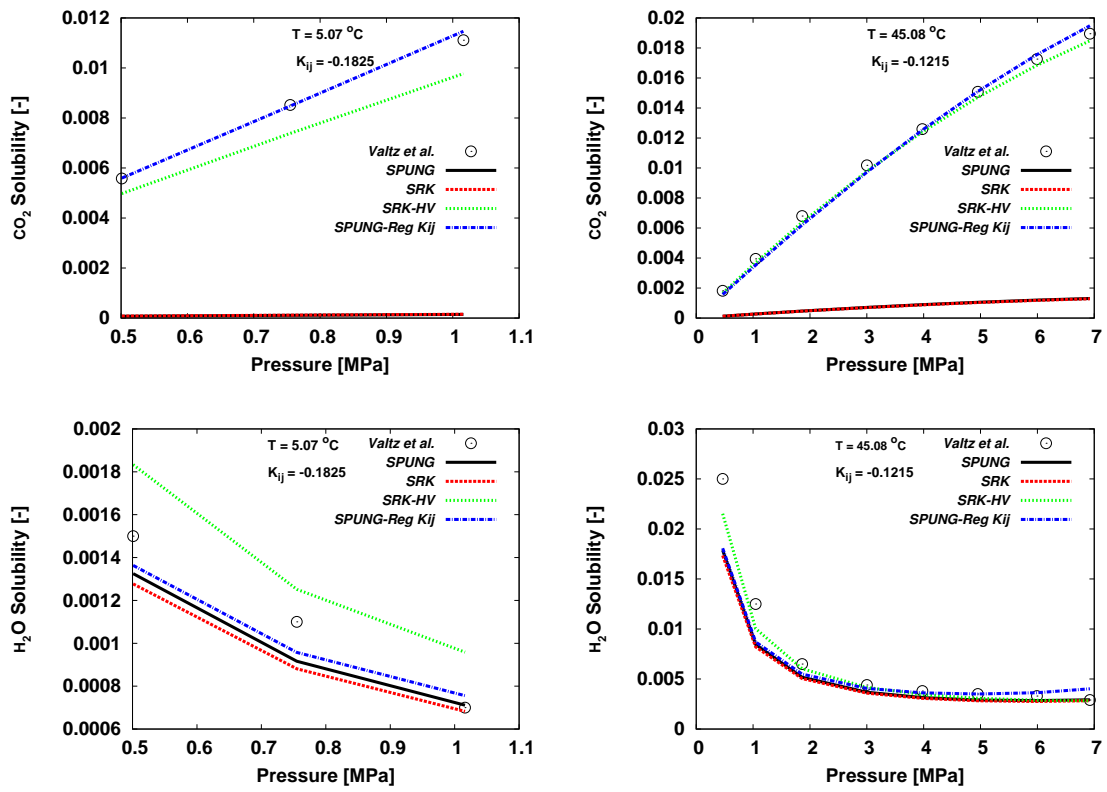


Figure 10: CO₂ and H₂O solubilities over low pressures and at temperatures of about 5 and 45 °C in comparison with Valtz et al. (2004) experimental data

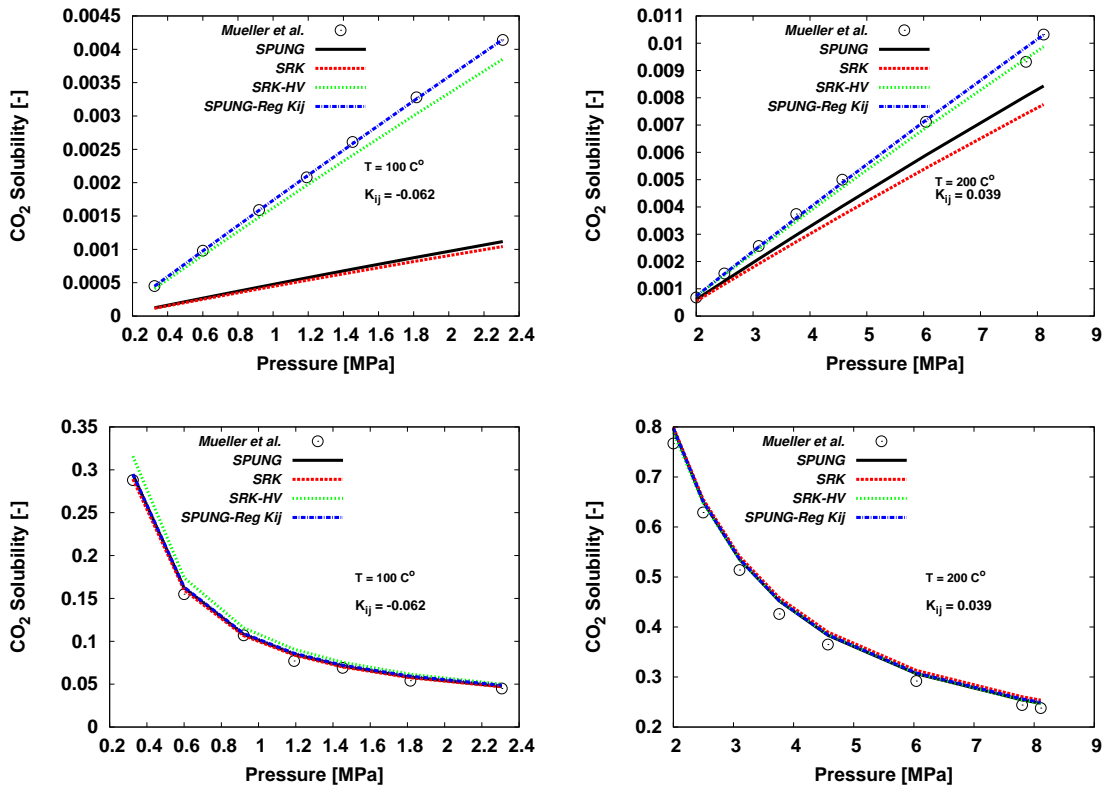


Figure 11: CO₂ and H₂O solubilities over low pressures and at temperatures of 100 and 200°C in comparison with Mueller et al. (1988) experimental data

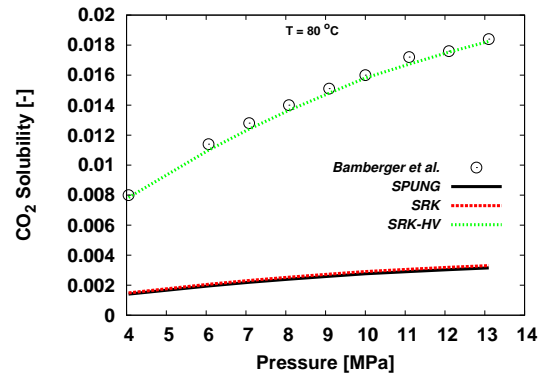


Figure 12: CO₂ solubilities over moderate pressures and at a temperature of 80 °C in comparison with Bamberger et al. (2000) experimental data

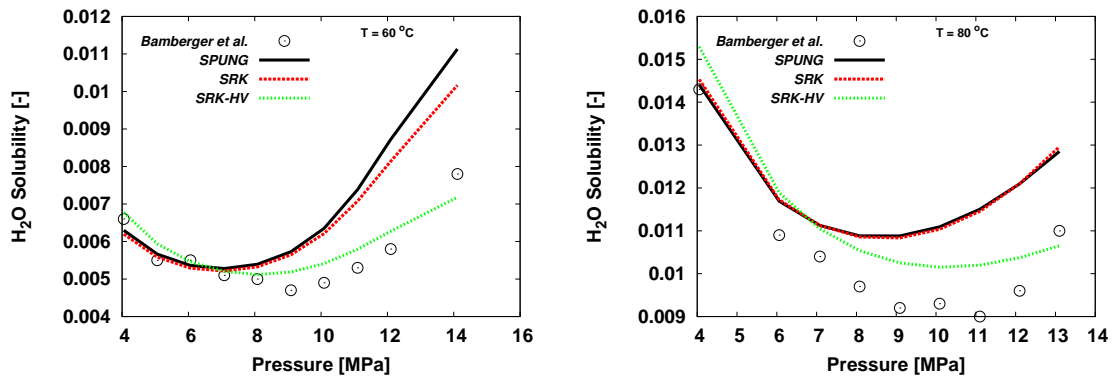


Figure 13: H_2O solubilities over moderate pressures and at temperatures of 60 and 80°C in comparison with Bamberger et al. (2000) experimental data

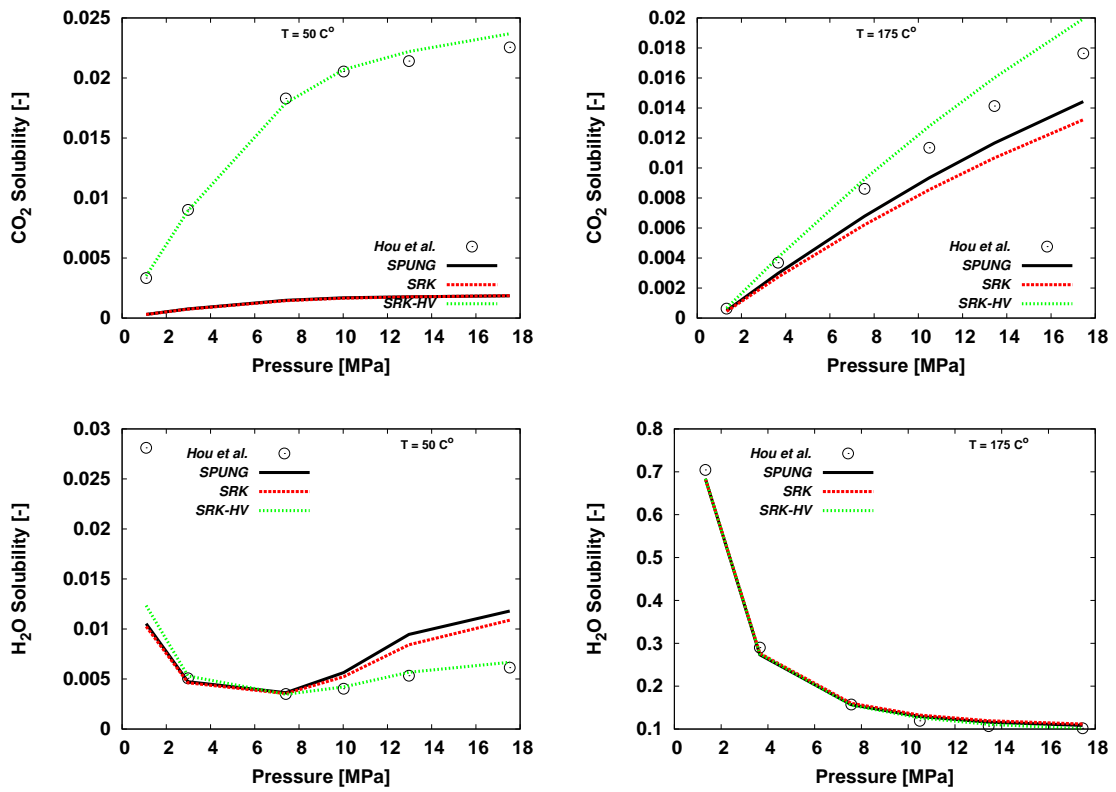


Figure 14: CO₂ and H₂O solubilities computations in comparison with experimental data of Hou et al. (2013)

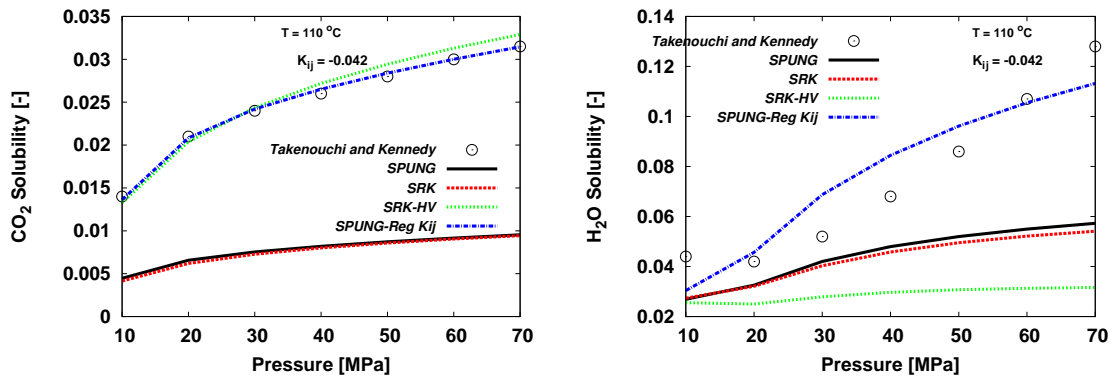


Figure 15: CO₂ and H₂O solubilities over very high pressures and a temperature of 110 °C in comparison with Takenouchi and Kennedy (1964) experimental data

Table 1: AAD [%] of the CO₂-rich phases density calculations for the CO₂-water system at different CO₂ co-existing phases and temperatures

Data sets	Phase Equilibrium	Temperature [°C]	SPUNG	SRK	SRK-HV	SPUNG-Reg	K_{ij}
<i>Chiquet et al. (2007)</i>	SGLE	35	1.8	8.3	8.7		4.5
		50	0.7	6.6	7.4		4.5
		90	4.5	6.9	8.2		7.1
		110	5.3	7.1	7.9		7.4
		90 ^a	2.7	5.3	6.7		5.7
		110 ^b	2.0	5.9	7.3		3.7
<i>Bikkina et al. (2011)^c</i>	LLE	25	2.0	9.2	9.7		8.3
<i>Bikkina et al. (2011)^c</i>	VLE		0.6	0.3	0.3		0.7

^a without the anomalous point 7.5 MPa, ^b without the anomalous point 25 MPa, ^c predicted data

Table 2: AAD [%] of Water rich liquid phase densities averaged over the temperatures of each evaluated set of data

Data sets	Phase Equilibrium	SPUNG	SRK	SRK-HV	SPUNG-Reg K_{ij}
<i>King et al. (1992)</i>	LLE	20.5	25.5	23.9	18.7
<i>Chiquet et al. (2007)</i>	SGLE	21.6	26.0	25.0	20.3
<i>Hebach et al. (2004)</i>	VLE	20.1	24.9	24.5	19.4

Table 3: AAD [%] of densities averaged over the temperatures of the comparison with Hebach et al. (2004) data using various reference fluids

Data set	Phase Equilibrium	N ₂	O ₂	C1	C2	NC4
<i>Hebach et al. (2004)</i>	VLE	25.7	24.8	24.8	21.8	18.9

Table 4: AAD [%] of the solubility of CO₂ and H₂O in comparison to Valtz et al. (2004)

Component	Temperature [°C]	SPUNG	SRK	SRK-HV	SPUNG-Reg K_{ij}
CO ₂	5.07	98.7	98.6	12.0	2.7
	25.13	96.8	96.7	8.8	5.5
	45.08	93.1	93.2	4.3	5.3
H ₂ O	5.07	10.0	12.4	24.3	10.0
	25.13	17.8	20.8	8.3	17.0
	45.08	17.5	18.9	10.4	16.8

Table 5: AAD [%] of the solubility of CO₂ and H₂O in comparison to Mueller et al. (1988)

Component	Temperature [°C]	SPUNG	SRK	SRK-HV	SPUNG-Reg K_{ij}
CO ₂	100	72.8	74.5	7.2	0.5
	140	49.2	53.2	4.9	1.1
	200	17.0	24.2	4.5	2.8
H ₂ O	100	4.9	3.6	11.8	6.3
	140	3.1	3.3	0.9	2.4
	200	4.5	6.1	4.4	4.9

Table 6: AAD [%] of the solubility of CO₂ and H₂O at different temperatures in comparison with Bamberger et al. (2000)

Component	Temperature [°C]	SPUNG	SRK	SRK-HV
CO ₂	50	91.8	91.7	2.1
	60	88.9	89.2	1.3
	80	82.8	81.9	2.0
H ₂ O	50	18.2	24.9	4.2
	60	20.5	17.1	6.2
	80	15.0	15.1	8.4

Table 7: AAD [%] of the solubility of CO₂ and H₂O at different temperatures in comparison with Wiebe (1941)

Component	Temperature [°C]	SPUNG	SRK	SRK-HV
CO ₂	50	92.0	91.8	6.9
	75	84.3	84.3	2.01
H ₂ O	50	167.9	157.9	33.1
	75	148.5	137.2	35.5

Table 8: AAD [%] of solubilities in comparison with Takenouchi and Kennedy (1964)

Component	SPUNG	SRK	SRK-HV	SPUNG-Reg K_{ij}
CO ₂	68.9	69.9	4.0	1.1
H ₂ O	36.2	38.3	56.5	17.3